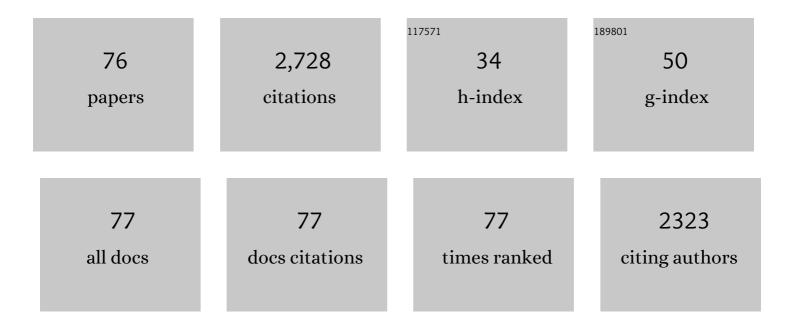
## Jialiang Gu

List of Publications by Year in descending order

Source: https://exaly.com/author-pdf/8312591/publications.pdf Version: 2024-02-01



#	Article	IF	CITATIONS
1	ANN-based structure-viscosity relationship model of multicomponent slags for production design in mineral wool. Construction and Building Materials, 2022, 319, 126010.	3.2	12
2	Investigation of cooling processes of molten slags to develop multilevel control method for cleaner production in mineral wool. Journal of Cleaner Production, 2022, 339, 130548.	4.6	7
3	Experimental Investigation of Vitrification Process for the Disposal of Hazardous Solid Waste Containing Chlorides. Processes, 2022, 10, 526.	1.3	0
4	Designing Structure–Thermodynamics-Informed Artificial Neural Networks for Surface Tension Prediction of Multi-component Molten Slags. Metallurgical and Materials Transactions B: Process Metallurgy and Materials Processing Science, 2022, 53, 2018-2029.	1.0	4
5	Preparation, Sintering Behavior and Consolidation Mechanism of Vanadium-Titanium Magnetite Pellets. Crystals, 2021, 11, 188.	1.0	11
6	Three-Stage Method Energy–Mass Coupling High-Efficiency Utilization Process of High-Temperature Molten Steel Slag. Metallurgical and Materials Transactions B: Process Metallurgy and Materials Processing Science, 2021, 52, 3004-3015.	1.0	7
7	Structural and Viscous Insight into Impact of MoO3 on Molten Slags. Metallurgical and Materials Transactions B: Process Metallurgy and Materials Processing Science, 2021, 52, 3730-3743.	1.0	11
8	Development of structure-informed artificial neural network for accurately modeling viscosity of multicomponent molten slags. Ceramics International, 2021, 47, 30691-30701.	2.3	16
9	Promoting Effect of Ti Species in MnOx-FeOx/Silicalite-1 for the Low-Temperature NH3-SCR Reaction. Catalysts, 2020, 10, 566.	1.6	8
10	Highly dispersed MnO <sub>x</sub> –FeO <sub>x</sub> supported by silicalite-1 for the selective catalytic reduction of NO <sub>x</sub> with NH <sub>3</sub> at low temperatures. Catalysis Science and Technology, 2020, 10, 5525-5534.	2.1	6
11	In Situ DRIFTS Investigation on CeOx Catalyst Supported by Fly-Ash-Made Porous Cordierite Ceramics for Low-Temperature NH3-SCR of NOX. Catalysts, 2019, 9, 496.	1.6	10
12	Insight into the Relationship Between Viscosity and Structure of CaO-SiO2-MgO-Al2O3 Molten Slags. Metallurgical and Materials Transactions B: Process Metallurgy and Materials Processing Science, 2019, 50, 2930-2941.	1.0	57
13	Kinetic studies on bituminous coal char gasification using CO <sub>2</sub> and H <sub>2</sub> O mixtures. International Journal of Green Energy, 2019, 16, 1144-1151.	2.1	11
14	Fabrication and characterization of porous cordierite ceramics prepared from fly ash and natural minerals. Ceramics International, 2019, 45, 18306-18314.	2.3	40
15	Reuse of mineral wool waste and recycled glass in ceramic foams. Ceramics International, 2019, 45, 15057-15064.	2.3	55
16	Synthesis of a foam ceramic based on ceramic tile polishing waste using SiC as foaming agent. Ceramics International, 2018, 44, 10078-10086.	2.3	62
17	Application of washed MSWI fly ash in cement composites: long-term environmental impacts. Environmental Science and Pollution Research, 2018, 25, 12127-12138.	2.7	29
18	Magnetic multi-metal co-doped magnesium ferrite nanoparticles: An efficient visible light-assisted heterogeneous Fenton-like catalyst synthesized from saprolite laterite ore. Journal of Hazardous Materials, 2018, 344, 829-838.	6.5	56

JIALIANG GU

#	ARTICLE	IF	CITATIONS
19	Roles of P <sub>2</sub> O <sub>5</sub> Addition on the Viscosity and Structure of CaO–SiO <sub>2</sub> –Al <sub>2</sub> O <sub>3</sub> –Na <sub>2&amp; Melts. ISIJ International, 2018, 58, 1644-1649.</sub>	l <b>t)/s</b> ub>	; <b>0â€"</b> P&lc
20	Recycling ground MSWI bottom ash in cement composites: Long-term environmental impacts. Waste Management, 2018, 78, 841-848.	3.7	46
21	Integrated utilization of high alumina fly ash for synthesis of foam glass ceramic. Ceramics International, 2018, 44, 13681-13688.	2.3	55
22	Long-term leaching behaviours of cement composites prepared by hazardous wastes. RSC Advances, 2018, 8, 27602-27609.	1.7	5
23	Solid wastes utilization in the iron and steel industry in China: towards sustainability. Institutions of Mining and Metallurgy Transactions Section C: Mineral Processing and Extractive Metallurgy, 2017, 126, 41-46.	0.6	8
24	Synthesis of a ceramic tile base based on high-alumina fly ash. Construction and Building Materials, 2017, 155, 930-938.	3.2	42
25	Promotional effect of rare earth-doped manganese oxides supported on activated semi-coke for selective catalytic reduction of NO with NH3. Environmental Science and Pollution Research, 2017, 24, 24473-24484.	2.7	23
26	Effect of water-washing on the co-removal of chlorine and heavy metals in air pollution control residue from MSW incineration. Waste Management, 2017, 68, 221-231.	3.7	62
27	Role of steel slags on biomass/carbon dioxide gasification integrated with recovery of high temperature heat. Bioresource Technology, 2017, 223, 1-9.	4.8	21
28	Integrated Utilization of Sewage Sludge and Coal Gangue for Cement Clinker Products: Promoting Tricalcium Silicate Formation and Trace Elements Immobilization. Materials, 2016, 9, 275.	1.3	17
29	A Fe-C-Ca big cycle in modern carbon-intensive industries: toward emission reduction and resource utilization. Scientific Reports, 2016, 6, 22323.	1.6	6
30	Effect of Al2O3 Addition on the Precipitated Phase Transformation in Ti-Bearing Blast Furnace Slags. Metallurgical and Materials Transactions B: Process Metallurgy and Materials Processing Science, 2016, 47, 1390-1399.	1.0	21
31	In situ DRIFTS studies on MnO nanowires supported by activated semi-coke for low temperature selective catalytic reduction of NO with NH3. Applied Surface Science, 2016, 366, 139-147.	3.1	71
32	Environmental investigation on co-combustion of sewage sludge and coal gangue: SO 2 , NO x and trace elements emissions. Waste Management, 2016, 50, 213-221.	3.7	108
33	Integration of coal gasification and waste heat recovery from high temperature steel slags: an emerging strategy to emission reduction. Scientific Reports, 2015, 5, 16591.	1.6	19
34	Coâ€pyrolysis characteristics of coal and sludge blends using thermogravimetric analysis. Environmental Progress and Sustainable Energy, 2015, 34, 1780-1789.	1.3	9
35	Facile and Economical Preparation of SiAlON-Based Composites Using Coal Gangue: From Fundamental to Industrial Application. Energies, 2015, 8, 7428-7440.	1.6	9
36	Co-modification and Crystalline-control of Ti-bearing Blast Furnace Slags. ISIJ International, 2015, 55, 158-165.	0.6	25

Jialiang Gu

#	Article	IF	CITATIONS
37	Enhancement of Rutile Formation by ZrO <sub>2</sub> Addition in Ti-bearing Blast Furnace Slags. ISIJ International, 2015, 55, 1384-1389.	0.6	7
38	Preparation and modeling of energy-saving building materials by using industrial solid waste. Energy and Buildings, 2015, 97, 6-12.	3.1	10
39	Integrated carbon dioxide/sludge gasification using waste heat from hot slags: Syngas production and sulfur dioxide fixation. Bioresource Technology, 2015, 181, 174-182.	4.8	53
40	Promoting effect of Nd on the reduction of NO with NH <sub>3</sub> over CeO <sub>2</sub> supported by activated semi-coke: an in situ DRIFTS study. Catalysis Science and Technology, 2015, 5, 2251-2259.	2.1	105
41	Co-combustion and emission characteristics of coal gangue and low-quality coal. Journal of Thermal Analysis and Calorimetry, 2015, 120, 1883-1892.	2.0	31
42	A Novel Kinematic Model for Molten Slag Fiberization: Prediction of Slag Fiber Properties. Metallurgical and Materials Transactions B: Process Metallurgy and Materials Processing Science, 2015, 46, 993-1001.	1.0	12
43	Achieving waste to energy through sewage sludge gasification using hot slags: syngas production. Scientific Reports, 2015, 5, 11436.	1.6	27
44	Heat Recovery from High Temperature Slags: A Review of Chemical Methods. Energies, 2015, 8, 1917-1935.	1.6	83
45	Facile and economical synthesis of porous activated semi-cokes for highly efficient and fast removal of microcystin-LR. Journal of Hazardous Materials, 2015, 299, 325-332.	6.5	17
46	Trace element partitioning behavior of coal gangue-fired CFB plant: experimental and equilibrium calculation. Environmental Science and Pollution Research, 2015, 22, 15469-15478.	2.7	29
47	Two-stage high temperature sludge gasification using the waste heat from hot blast furnace slags. Bioresource Technology, 2015, 198, 364-371.	4.8	45
48	Effects of chemistry and mineral on structural evolution and chemical reactivity of coal gangue during calcination: towards efficient utilization. Materials and Structures/Materiaux Et Constructions, 2015, 48, 2779-2793.	1.3	48
49	Effect of P2O5 Addition on the Viscosity and Structure of Titanium Bearing Blast Furnace Slags. ISIJ International, 2014, 54, 1491-1497.	0.6	23
50	Effect of B2O3 on the Structure and Viscous Behavior of Ti-Bearing Blast Furnace Slags. Jom, 2014, 66, 2168-2175.	0.9	55
51	Multi-Stage Control of Waste Heat Recovery from High Temperature Slags Based on Time Temperature Transformation Curves. Energies, 2014, 7, 1673-1684.	1.6	42
52	Characteristics of low temperature biomass gasification and syngas release behavior using hot slag. RSC Advances, 2014, 4, 62105-62114.	1.7	36
53	Pyrite transformation and sulfur dioxide release during calcination of coal gangue. RSC Advances, 2014, 4, 42506-42513.	1.7	27
54	In situ DRIFTS investigation on the SCR of NO with NH3 over V2O5 catalyst supported by activated semi-coke. Applied Surface Science, 2014, 313, 660-669.	3.1	145

JIALIANG GU

#	Article	IF	CITATIONS
55	Investigation of the Viscosity and Structural Properties of CaO-SiO2-TiO2 Slags. Metallurgical and Materials Transactions B: Process Metallurgy and Materials Processing Science, 2014, 45, 1389-1397.	1.0	99
56	The Effect of P2O5 on the Crystallization Behaviors of Ti-Bearing Blast Furnace Slags Using Single Hot Thermocouple Technique. Metallurgical and Materials Transactions B: Process Metallurgy and Materials Processing Science, 2014, 45, 1446-1455.	1.0	40
57	Low-temperature SCR of NO with NH3 over activated semi-coke composite-supported rare earth oxides. Applied Surface Science, 2014, 309, 1-10.	3.1	71
58	Tailoring CoO–ZnO nanorod and nanotube arrays for Li-ion battery anode materials. Journal of Materials Chemistry A, 2013, 1, 9654.	5.2	59
59	Activated Semi-coke in SO <sub>2</sub> Removal from Flue Gas: Selection of Activation Methodology and Desulfurization Mechanism Study. Energy & Fuels, 2013, 27, 3080-3089.	2.5	78
60	Influence of Basicity and TiO2 Content on the Precipitation Behavior of the Ti-bearing Blast Furnace Slags. ISIJ International, 2013, 53, 1696-1703.	0.6	50
61	Effect of Substrate Pretreatment on Controllable Growth of TiO2 Nanorod Arrays. Journal of Materials Science and Technology, 2012, 28, 577-586.	5.6	20
62	Ultrasensitive sorption behavior of isostructural lanthanide–organic frameworks induced by lanthanide contraction. Journal of Materials Chemistry, 2012, 22, 21076.	6.7	48
63	Conductivity properties of Î <sup>2</sup> -SiAlON ceramics. Science China Technological Sciences, 2012, 55, 2409-2415.	2.0	7
64	Pore size-controlled gases and alcohols separation within ultramicroporous homochiral lanthanide–organic frameworks. Journal of Materials Chemistry, 2012, 22, 7813.	6.7	53
65	Effect of Al <sub>2</sub> O <sub>3</sub> /SiO <sub>2</sub> Ratio on the Viscosity and Structure of Slags. ISIJ International, 2012, 52, 753-758.	0.6	90
66	Crystallization Behavior of Rutile in the Synthesized Ti-bearing Blast Furnace Slag Using Single Hot Thermocouple Technique. ISIJ International, 2011, 51, 1396-1402.	0.6	58
67	The Influence of SiO <sub>2</sub> on the Extraction of Ti Element from Tiâ€bearing Blast Furnace Slag. Steel Research International, 2011, 82, 607-614.	1.0	55
68	Effects of pretreatment of substrates on the preparation of large scale ZnO nanotube arrays. Rare Metals, 2010, 29, 21-25.	3.6	3
69	Hydrothermal growth of well-aligned TiO2 nanorod arrays: Dependence of morphology upon hydrothermal reaction conditions. Rare Metals, 2010, 29, 286-291.	3.6	40
70	Studies on the PEG-Assisted Hydrothermal Synthesis and Growth Mechanism of ZnO Microrod and Mesoporous Microsphere Arrays on the Substrate. Crystal Growth and Design, 2010, 10, 1500-1507.	1.4	60
71	Calculations of Freezing Point Depression, Boiling Point Elevation, Vapor Pressure and Enthalpies ofÂVaporization of Electrolyte Solutions by a Modified Three-Characteristic Parameter Correlation Model. Journal of Solution Chemistry, 2009, 38, 1097-1117.	0.6	22
72	Thermodynamic study and syntheses of β-SiAlON ceramics. Science in China Series D: Earth Sciences, 2009, 52, 3122-3127.	0.9	9

JIALIANG GU

#	Article	IF	CITATIONS
73	Preparation and properties of a nano TiO2/Fe3O4 composite superparamagnetic photocatalyst. Rare Metals, 2009, 28, 423-427.	3.6	78
74	Template-free hydrothermal synthesis of single-crystalline SnO2 nanocauliflowers and their optical properties. Rare Metals, 2009, 28, 449-453.	3.6	6
75	Activity of VO1.5 in CaO-SiO2-MgO-Al2O3 Slags at Low Vanadium Contents and Low Oxygen Pressures. , 2009, 80, 251.		4
76	The Preparation and Characterization of <mml:math xmlns:mml="http://www.w3.org/1998/Math/MathML"&gt;<mml:mi mathvariant="bold"&gt;β-SiAION Nanostructure Whiskers. Journal of Nanomaterials, 2008, 2008, 1-6.</mml:mi </mml:math 	1.5	18